THE EFFECTS OF INFALL AND SOURCE EVOLUTION ON THE CHEMISTRY OF MASSIVE STAR-FORMNIG REGIONS. S. D. Doty[1], E. F. van Dishoeck[2], and J. C. Tan[3], [1]Department of Physics and Astronomy, Denison University, Granville, OH 43023, USA (doty@denison.edu), [2]Sterrewacht Leiden, PO Box 9513, 2300 RA Leiden, The Netherlands, [3]Princeton University Observatory, Peyton Hall, Princeton, NJ 08544, USA.

Introduction: The physical and chemical structure of young stellar objects (YSOs) has been an area of increasing study, driven by multi-wavelength observations, smaller (15'') submillimeter beams, interferometry, and the use of satellites to probe spectral regions inaccessible from the ground. These data are then combined with detailed chemical evolution and radiative transfer models to infer the source properties. In the case of low-mass YSOs, evolutionary models have had recent success [1,2,3]. For massive YSOs, static gas-phase chemical models combined with physical structure have been applied to a wide range of molecular line observations to constrain properties such as the cosmic-ray ionization rate, time since source turn-on, and CO ad/desorption [4]. Of significant interest is the use of multi-wavelength observations [5] to parametrically constrain the water vapor distribution. In order to remove the limiting static and gas-phase assumptions, we have present the first time- and depth-dependent models of the envelopes of massive YSOs in which a realistic evolution of the source and infall of the gas and dust, and in which the gas-grain ad/desorption is incorporated consistently with recent laboratory measurements.

Model: For concreteness, we concentrate our model on the outer envelope of the well-observed, relatively isolated YSO AFGL 2591, though past experience leads us to believe that the results will be generally applicable to other sources. For simplicity, we assume spherical symmetry.

Physical structure and evolution. The physical structure was constrained [6,7] to be well-described by a power law density distribution of the form $n(r) = n_0 (r_0/r)^m$, where m ~ 1 – 1.5. The polytropic dynamics and central source evolution are based upon a recent model of massive core collapse [8]. Since the polytropic evolution diverges for m = 1, we adopt m = 1.1.

Chemistry. The gas-phase chemistry is based upon the existing static chemical model [4], where the initial conditions are consistent with a cold cloud near T ~ 10K. We include ad/desorption of species to/from dust grains, including the recent Temperature Programmed Desorption (TPD) laboratory work [9,10].

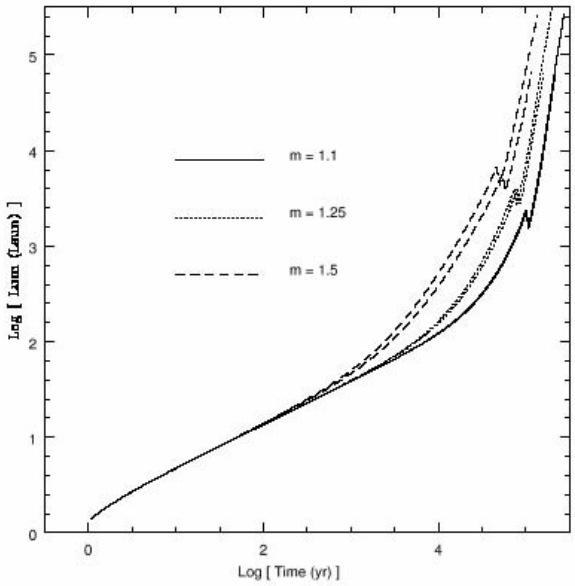

Figure 1. The luminosity of the central YSO for AFGL 2591 as a function of time for the massive core collapse model of [8]. The different line types correspond to different density distribution power laws (m; see text). For each line type, the lower and upper curves represent a final stellar mass $M_{*,f}$ = 20 and 40 M_{sun} respectively.

Results:

Physical evolution. As described above, the density distribution is given roughly by a power-law with index m ~ 1.1. The resulting central luminosity of the YSO as a function of time is shown in Fig. 1 for a range of density distribution indicies (m = 1.1, 1.25, 1.5), and for two different values of the final stellar mass ($M_{*,f}$ =20, 40 M_{sun}). Notice that L(t) does not depend significantly on m or $M_{*,f}$, only varying by a factor of ~ 2x. This results in a negligible difference in temperature, as $T(r) \sim T_0 L^{1/6}$ for reasonable grains [11], leading to $\Delta T / T \sim 12\%$ for $\Delta L / L \sim 2$. Given the density and luminosity functions, we utilize an adopted set of grain properties [12], and dust radiative transfer model [13] to determine the time- and depth-dependent temperature distribution. The results are shown in Fig. 2, where the warming due to the evolution of the YSO is apparent. Given the high densities, we assume that the gas and dust are well-coupled so that $T_{gas} \sim T_{dust}$ [14].

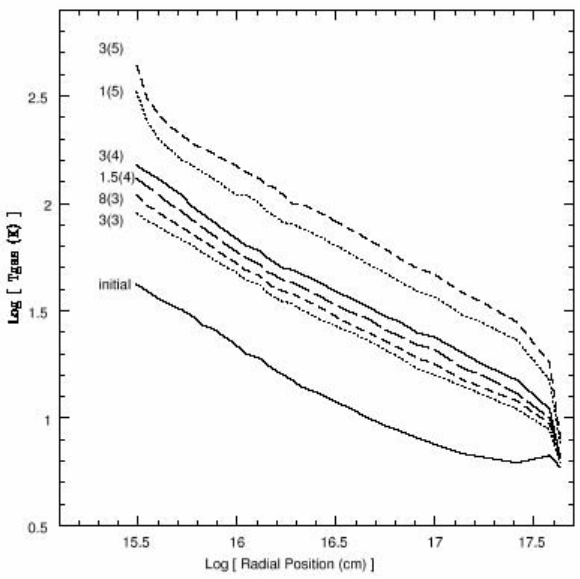

Figure 2. The dust temperature distribution as a function of position for various times. The curves are labeled by the time in years since formation of the core, where A(B) means A x 10^B years.

Chemical evolution. Previous detailed chemical and radiative transfer modeling [4,5] were able to parametrically constrain the water vapor distribution, and led to three main conclusions: (1) water evaporates from the ice mantles at T ~ 100K, or r ~ $10^{16\text{-}16.5}$ cm; (2) $x(H_2O)_{T>100} = n(H_2O)_{T>100} / n(H_2)_{T>100} = 2 \times 10^{-4}$; and (3) $x(H_2O)_{T<100} < 10^{-8}$. When we include infall, source evolution, and detailed mantle ad/desorption, the grain mantles desorb as the source warms the dust and gas, and as the grains fall into the warmer interior. The resulting gas-phase water abundance distribution is shown in Fig. 3. The lines are the model abundance profiles for various times. The abundance constraints are given by the cross-hatched regions, while the location of the parametric evaporation step is noted by the double arrows. It is remarkable that the step-function distribution adopted in the parametric studies is naturally reproduced by the combination of source evolution, infall, and grain mantle evaporation. Quantiatively, we see that for $t < 3 \times 10^4$ yrs the inner abundances is too small / the location of the evaporation step is too interior to be consistent with the observations, due to the fact that the source is not yet luminous enough to have evaporated the models. On the other hand, for $t > 10^5$ yrs, the outer abundance is too high. This is due to the further evaporation of the mantles as the source continues to warm. The water near 10^{16} cm is removed by cosmic-ray produced ions (e.g. H_3^+, HCO^+, N_2H^+). The oxygen is efficiently shuttled into O_2 via dissociative recombination of H_3O^+ into OH followed by reactions with O, and into CO_2 by reactions of CO with OH. In the very interior, the water abundance is still high due to the fast reaction of OH with H_2 to form H_2O with an activation energy of ~ 1600K. This combination nicely brackets the observational constraints. Physically, it suggests that the source has had sufficient time to warm the interior and liberate water, but not so much time as to warm the entire envelope or produce significant ion-molecule chemistry. Furthermore, Fig. 3 suggests an age of 3 – 10 x 10^4 yrs since the formation of the protostar – roughly consistent with previous gas-phase chemical modeling [4].

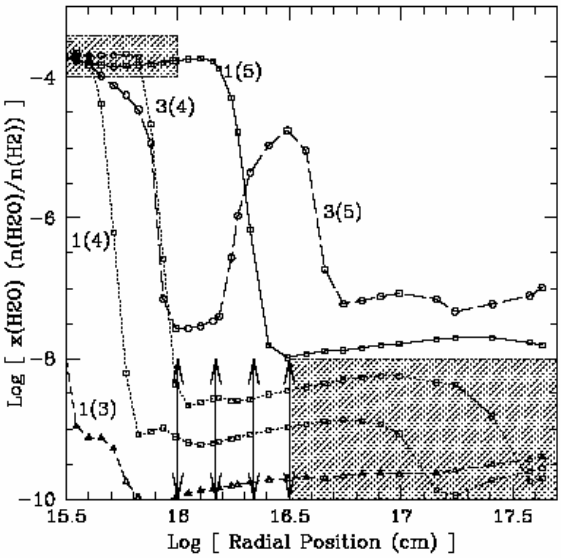

Figure 3. Water distribution for various times since protostellar formation. Observational constraints are given by the cross-hatched regions, and the constraint for the "step" by the double arrows.

References:

[1] Rodgers S. D. and Charnley S. B (2003) ApJ, *585*, 355-371. [2] Viti S. and Williams D. A. (1999) MNRAS, *305*, 755-762 [3] Lee J.-E., Bergin E. A., and Evans N. J. (2004) ApJ, *617*, 360-383. [4] Doty S. D., van Dishoeck E. F., van der Tak F. F. S. and Boonman A. M. S. (2002) A&A, *386*, 446-463. [5] Boonman A. M. S. (2003) A&A, *406*, 937-955. [6] van der Tak F. F. S. et al. (1999) ApJ, *522*, 991-1010. [7] van der Tak F. F. S. et al. (2000) ApJ, *537*, 283-303. [8] McKee C. and Tan J. (2003) ApJ, 585, 850-871. [9] Fraser H. et al. (2001) MNRAS, *327*, 1165-1172. [10] Collings M. P. et al. (2003) ApJ, *583*, 1058-1062. [11] Doty S. D. and Leung C. M. (1994) ApJ, *424*, 729-747. [12] Ossenkopf V. and Henning Th. (1994) A&A, *291*, 943-959. [13] Egan M. P., Leung C. M., and Spagna G. F. (1988) CoPhComm, *48*, 271-292. [14] Doty S. D. and Neufeld D. A. (1997) ApJ, *489*, 122-142.